

New physics contamination to precision luminosity measurements at future e^+e^- colliders

Mauro Chiesa,^{1,*} Clara L. Del Pio,^{2,†} Guido Montagna,^{3,1,‡}
Oreste Nicosini,^{1,§} Fulvio Piccinini,^{1,¶} and Francesco P. Ucci^{3,1,**}

¹*INFN, Sezione di Pavia, Via A. Bassi 6, 27100 Pavia, Italy*

²*Department of Physics, Brookhaven National Laboratory, Upton, New York 11973, USA*

³*Dipartimento di Fisica "Alessandro Volta", Università di Pavia, Via A. Bassi 6, 27100 Pavia, Italy*

Several key observables of the high-precision physics program at future lepton colliders will critically depend on the knowledge of the absolute machine luminosity. The determination of the luminosity relies on the precise knowledge of some reference process, which is, in principle, not affected by unknown physics, so that its cross section can be computed within a well-established theory, like the Standard Model. Quantifying the uncertainties induced by possible New Physics effects on such processes is, therefore, crucial. We present an investigation of light and heavy new physics contributions to the small-angle Bhabha process at future e^+e^- colliders and we discuss possible strategies to remove the contamination due to heavy degrees of freedom by relying on observables that are independent of the absolute luminosity.

I. INTRODUCTION

The absolute luminosity measurement is extremely important at e^+e^- colliders, from low to high energy, because it is a source of systematics in the measurement of the cross section of signal processes. For instance, at the few-GeV scale of flavor factories, it is crucial for the determination of the pion form factor through the measurement of the hadronic cross section in e^+e^- collisions [1], while at the energies of Z factories, like LEP in the past and at Higgs, top and electroweak factories in the future [2], it is relevant for the determination of some key Standard Model (SM) parameters [3–5]. An example of the importance of a precise knowledge of the absolute luminosity is given by the recent study of the effects of beam-beam interactions at LEP [4], where an underestimate of the LEP luminosity of about 0.1% was discovered, removing a long-standing tension on the number of light neutrino species from LEP [5].

At future e^+e^- high energy colliders, the luminosity calibration will also play a crucial role in improving the precision of electroweak (EW) measurements. For instance, an uncertainty of 10^{-4} on the luminosity at WW threshold would allow the precise knowledge of the W mass and width with a 0.3 and 1.2 MeV statistical precision respectively, through the measurement of the W -pair cross section line shape [6, 7]. Moreover, an unprecedented precision on the effective HZZ coupling and the total Higgs boson width through the measurement of the total cross section of the process $e^+e^- \rightarrow HZ$ at energy scales above the HZ threshold could be achieved if the

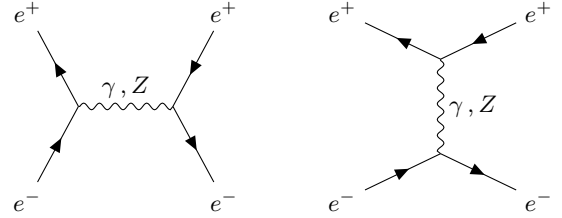


FIG. 1. Tree level s - and t -channel diagrams for the Bhabha scattering.

systematic error due to luminosity is kept small, in order to fully exploit the achievable statistics.

The time-integrated luminosity L is related to the cross section σ_0 of some reference process through the relation

$$L = \int \mathcal{L} dt = \frac{N_0}{\epsilon \sigma_0}, \quad (1)$$

where \mathcal{L} is the instantaneous luminosity, N_0 is the number of observed events of such a process and ϵ is the experimental selection efficiency. On the one hand, the choice of the reference processes is motivated by clean experimental signatures and large cross sections, in order to minimise the experimental systematics. On the other hand, a further important requirement is the feasibility of a very precise theoretical description of the differential cross sections of the reference process, since the precision in the cross section calculation enters directly as a source of systematics. At LEP, the above conditions were satisfied by small angle Bhabha scattering (SABS), where the process is largely dominated by the QED photon exchange and the imperfect knowledge of the weak interactions has not been a matter of concern. This can be understood by looking at the angular dependence of the SABS cross section differential in the electron scattering

* mauro.chiesa@pv.infn.it

† cdelpio@bnl.gov

‡ guido.montagna@unipv.it

§ oreste.nicosini@pv.infn.it

¶ fulvio.piccinini@pv.infn.it

** francesco.ucci@pv.infn.it

angle that is given by

$$\frac{d\sigma_0}{d\theta} = \frac{32\pi\alpha^2}{s\theta^3} \left(1 - \frac{\theta^2}{2} + \frac{9}{40}\theta^4 + \delta_{\text{weak}} \right), \quad (2)$$

where the $1/\theta^3$ behavior is due to the photon t -channel diagram shown in the right panel in Fig. 1 and s is the center of mass (c.m.) energy. In the LEP luminometer acceptance, the contribution due to the Z exchange was at most $\delta_{\text{weak}} \sim 0.3\%$ [8], with its radiative corrections being at the level of 10^{-4} . At flavor factories, the main reference process is the large-angle Bhabha scattering (LABS) [1] and the processes $e^+e^- \rightarrow \mu^+\mu^-$ and $e^+e^- \rightarrow \gamma\gamma$ are also used for normalization and cross-checks.

The highest relative experimental precision in the absolute luminosity calibration was achieved by the OPAL Collaboration [9] at LEP, with the value of 3.4×10^{-4} . Such a high level of precision was matched by theoretical predictions via the inclusion of exact next-to-leading-order (NLO) calculations and the resummation of higher-order photon emissions [10]. At future e^+e^- high-energy colliders, the precision requirements for the luminosity measurements will be even more demanding, being of the order of at least 10^{-4} , or possibly better, at the Z resonance and at the WW threshold region, and of the order of 10^{-3} at c.m. energies larger than about 240 GeV [11]. On the theoretical side, studies on the needs for the SM calculations and Monte Carlo event generators to reach such unprecedented precisions have appeared recently in the literature [12–18]. While this outlines a clear program for improving SM calculations, for example including also NLO weak corrections, the impact of new physics (NP) on luminosity measurements remains less explored. An unknown degree of freedom (d.o.f.) could contribute to the benchmark process cross section, potentially biasing absolute cross section determinations or at least increasing the associated theoretical uncertainty.

In this paper, we investigate whether NP could contaminate the absolute luminosity measurements at various future high-energy e^+e^- colliders proposals through SABS, using the present and projected knowledge of the bounds on beyond the Standard Model (BSM) effects. A complementary investigation in this direction was presented in [19] for the process $e^+e^- \rightarrow \gamma\gamma$, which is presently under consideration as an alternative luminosity process [11, 20, 21], highlighting the interplay between higher-dimension NP effects and FCC-ee luminosity measurements. Additionally, we explore the effectiveness of the asymmetry measurements of LABS as a tool to remove the uncertainties due to possible NP contributions.

II. NEW PHYSICS IMPACT ON SABS

The NP contribution to the SABS cross section can be due to heavy new d.o.f. or to light mediators with feeble couplings to the leptons or photons which have es-

caped detection until now. For the former case, the natural framework for a model-independent analysis is the Standard Model effective field theory (SMEFT), where all possible higher-dimensional operators are added to the SM Lagrangian. For the latter case of light NP contributions, a model-dependent analysis is necessary. We will, therefore, study the effects due to the exchange of light d.o.f. with spin 0 or 1 and with different parity.

We consider in this analysis various future e^+e^- collider options, in particular FCC [22–24], CEPC [25, 26], ILC [27–32], and CLIC [33–36]. The typical angular acceptances of the luminometers [37] and c.m. energies of the colliders are specified in the second and third columns in Table II, respectively. For the EW sector, we adopt the $\{\alpha(M_Z), G_\mu, M_Z\}$ input parameter scheme with the following numerical values

$$\begin{aligned} \alpha(M_Z) &= 1/127.95 \\ G_\mu &= 1.16638 \times 10^{-5} \text{ GeV}^{-2} \\ M_Z &= 91.1876 \text{ GeV} . \end{aligned}$$

The relevant amplitudes have been generated with FEYNARTS [38] and FEYNALC [39, 40]. For the SMEFT, we have used the UFO [41] model from SMEFTFR [42–44] and checked against SMEFTSIM [45, 46] within MG5_AMC@NLO [47], while the UFO used for light NP has been obtained by implementing the Lagrangians in FEYNRULES [48] and used as model files in FEYNARTS.

Numerical results have been obtained with an updated version [49] of the BABAYAGA@NLO Monte Carlo generator [50–54], able to simulate the Bhabha scattering with NLO QED corrections matched to a parton shower for γ and Z exchange. The latest version includes NP effects for light and heavy mediators as described in the following.

A. Light new physics scenarios

If the mass of NP is below the EW scale, i.e. $M_{\text{NP}} \lesssim \Lambda_{\text{EW}}$, an EFT approach is not suitable and we need to rely on specific renormalizable models. Inspired by [55], we analyze the maximal contamination of couplings of SM particles to (pseudo)scalar, (axial)vector NP d.o.f. that are not excluded by the current experimental bounds. As shown in the following, the numerical results obtained with BABAYAGA@NLO, for processes interfering with the SM, can be understood by considering the analytical estimate of the leading light NP (LNP) deviations given by

$$\delta_{\text{LNP}} \simeq \frac{2 \text{Re}(\mathcal{M}_\gamma(t)^\dagger \mathcal{M}_{\text{LNP}})}{|\mathcal{M}_\gamma(t)|^2}, \quad (3)$$

where the subscript γ indicates the photon exchange, which dominates the SM SABS amplitude in the t channel, whereas \mathcal{M}_{LNP} is the amplitude for the considered

light NP models, whose relevant Feynman diagrams are represented in Fig. 2.

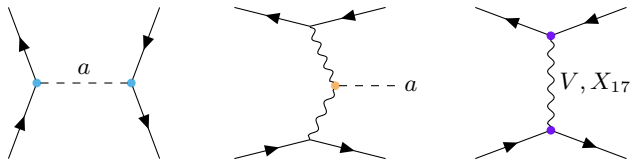


FIG. 2. Diagrams for LNP contributions to SABS. To the left and right, the t -channel diagram mediated either by a scalar or a dark vector, respectively. The central diagram represents the photon-photon fusion producing a light ALP in the final state. Dotted vertices correspond to LNP couplings, indicated by colors.

1. (Pseudo)scalar axionlike particles

The interaction of a (pseudo)scalar axionlike particle (ALP) a of mass m_a with both the photon and the electron can be parametrized with the parity-violating Lagrangian

$$\begin{aligned} \mathcal{L}_{\text{ALP}} = & \frac{1}{2} \partial_\mu a \partial^\mu a - \frac{1}{2} m_a^2 a^2 \\ & + \frac{1}{4} g_{a\gamma\gamma} (F_{\mu\nu} \tilde{F}^{\mu\nu}) a + g_{aee} (\bar{e} i \gamma_5 e) a, \end{aligned} \quad (4)$$

where $F_{\mu\nu}$ is the electromagnetic field tensor, $\tilde{F}^{\mu\nu}$ the dual field tensor and e the electron field. In Eq. 4, the scalar parity-conserving case is obtained with the substitutions $\tilde{F}^{\mu\nu} \rightarrow F^{\mu\nu}$, $i\gamma_5 \rightarrow \mathbb{1}$. In the limit $m_a \ll \sqrt{s}$, the leading contribution in the axion-to-electron coupling g_{aee} is given by the interference of the t -channel photon exchange with the s -channel diagram mediated by the ALP, as $\mathcal{M}_\gamma^\dagger(t) \mathcal{M}_a(t)$ vanishes in the limit $m_e \simeq 0$, yielding a relative differential deviation given by

$$\delta_{\text{ALP}}^{aee} \simeq \frac{g_{aee}^2}{4\pi\alpha} \frac{s^2 t}{(s - m_a^2)(s^2 + u^2)} \simeq -\frac{g_{aee}^2}{8\pi\alpha} (1 - \cos\theta), \quad (5)$$

which is highly suppressed at small angle.

In order to evaluate the maximal effect, we consider the bounds put by the NA64 beam-dump experiment via the detection of missing energy in the hard bremsstrahlung process $e^- Z \rightarrow e^- Z X$; $X \rightarrow \text{invisible}$ [56] where X can have different intrinsic spin. In the unconstrained mass-coupling plane, we take the point with the largest value of the coupling of electrons to the axion, given by $(g_{aee}, m_a) \simeq (3 \times 10^{-3}, 1 \text{ GeV})$. At small angle, this yields $\delta_{\text{ALP}}^{aee} < 10^{-7}$, well below any future collider precision goal. A light ALP can be also produced via photon fusion in the process $e^+ e^- \rightarrow \gamma^* \gamma^* e^+ e^- \rightarrow e^+ e^- a$, shown in the middle panel in Fig. 2, that can give the same experimental signature of SABS [57]. For this process, the results have been obtained with a modified version of the code developed for simulating $\pi^0 \pi^0$ [58] and

η [59] production in $e^+ e^-$ collisions and π^0 production in μe scattering [60]. For the largest admitted value of the photon-axion coupling $g_{a\gamma\gamma} = 2 \times 10^{-4} \text{ GeV}^{-1}$ obtained via beam-dump experiments and invisible decay searches, as reported in Ref. [57] and references therein, this contribution at the Z peak in a small angular acceptance is suppressed, giving $\delta_{\text{ALP}}^{a\gamma\gamma} \sim \mathcal{O}(10^{-6})$. At higher energy, the bulk of the axion emission cross section is unchanged [61], while the SM cross section falls as $1/s$, yielding $\delta_{\text{ALP}}^{a\gamma\gamma}(1 \text{ TeV}) \sim \mathcal{O}(10^{-5})$. This feature can be understood since the total cross section for axion emission grows logarithmically with the c.m. energy [61] but the angular distribution of the electron and positron around the beam axis becomes more sharply peaked. The fixed angular acceptance effectively removes the increase of the cross section at high energies.

2. Dark vectors

In a light NP scenario, Bhabha scattering could also be mediated by a dark vector boson V_μ associated with a new $U(1)'$ gauge symmetry, usually referred to as dark photon [62] or light Z' models [63]. The kinetic mixing of such boson [64–66] with the SM (un)broken $U(1)_{(\text{em})Y}$ gauge field would result in a coupling with the electromagnetic current after the EW symmetry breaking. The Lagrangian we use to estimate such effects is given by

$$\begin{aligned} \mathcal{L}_{\text{Dark}} = & -\frac{1}{4} V^{\mu\nu} V_{\mu\nu} + \frac{1}{2} M_V^2 V_\mu V^\mu \\ & + g'_V (\bar{e} \gamma^\mu e) V_\mu + g'_A (\bar{e} \gamma^\mu \gamma_5 e) V_\mu, \end{aligned} \quad (6)$$

where $g'_{V,A}$ are the vector and axial couplings of the dark spin-1 mediator of mass M_V with electrons and $V_{\mu\nu}$ is the dark field tensor. The bulk of the deviation with respect to the SABS in the SM due to the V_μ mediator is given by the interference of the QED amplitude with the dark vector t -channel exchange, shown in the rightmost panel of Fig. 2, i.e.

$$\delta_{\text{Dark}} \simeq \frac{t \left[g_V'^2 (s^2 + u^2) - g_A'^2 (s^2 - u^2) \right]}{2\pi\alpha (t - M_V^2) (s^2 + u^2)}. \quad (7)$$

At small angles, one has $u \simeq -s$, resulting in a strongly suppressed axial-vector coupling. Bounds on g'_V are taken from the BABAR search for dark photons [67] via the process $e^+ e^- \rightarrow \gamma V$; $V \rightarrow \text{invisible}$, which are found to be more constraining than [56] in the region of $M_V \simeq 1 \text{ GeV}$. Therefore, the maximal contribution of the dark vector current is given for $(g'_V, M_V) \simeq (3 \times 10^{-4}, 1 \text{ GeV})$, resulting in $\delta_{\text{Dark}} \sim \mathcal{O}(10^{-6})$, which is 2 orders of magnitude below the foreseen luminosity precision of future colliders.

3. The hypothetical X_{17} particle

The anomalous resonance observed by the ATOMKI experiment [68] in ${}^8\text{Be}^* \rightarrow {}^8\text{Be} e^+ e^-$ nuclear transitions at $m_{e^+e^-} \simeq 17$ MeV has been interpreted as a new vector gauge boson [69]. Subsequent results with ${}^4\text{He}$ [70] and ${}^{12}\text{C}$ [71] atoms confirmed such findings, while the MEG II experiment [72] has not found evidence in its data, yet still being compatible with the existence of the X_{17} boson. Recently, the PADME experiment observed an excess e^+e^- data [73], by searching the resonant production and decay $X_{17} \rightarrow e^+e^-$ via a fixed target experiment, being compatible with the ATOMKI average. The experimental findings have been reviewed in detail in Ref. [74] while their phenomenological implications have been studied in [75, 76], but no consensus has been reached in the literature on the parity of the X_{17} coupling to electrons. Therefore, we parametrize the effect of the possible X_{17} mediation in the SABS with the (axial)vector Lagrangian of Eq. (6). We consider the most recent constraints from the PADME experiment that do not exclude the values $(g_{Xee}, m_X) = (5.6 \times 10^{-4}, 16.90 \text{ MeV})$. We find that the deviations due to the X_{17} in the SABS for the FCC-ee setup at $\sqrt{s} = M_Z$ are of the order of $\delta_{X_{17}} \simeq 6 \times 10^{-6}$, while at higher energies its effect is below the luminosity precision target. More data are foreseen in the next years that will shed light on the hypothetical X_{17} particle allowing for a precise estimation of the uncertainties to the SABS associated with it.

We can conclude that no contribution from light NP is expected to alter the SM picture of the SABS cross section at 10^{-4} level, allowing us to neglect such effects in the rest of this work.

B. Heavy new physics scenarios

Under the assumption that the NP scale lies far above the electroweak scale, i.e. $\Lambda_{\text{NP}} \gtrsim \mathcal{O}(\text{TeV})$, one can study deviations from the SM using the SMEFT framework at dimension six (see Ref. [77] for a review), a model-independent way to capture the leading BSM effects. The effective Lagrangian is expanded about the SM as follows

$$\mathcal{L}_{\text{SMEFT}} = \mathcal{L}_{\text{SM}} + \sum_i \frac{C_i \hat{O}_i^{(6)}}{\Lambda_{\text{NP}}^2} + \mathcal{O}\left(\frac{1}{\Lambda_{\text{NP}}^4}\right), \quad (8)$$

where the operators $\hat{O}_i^{(6)}$ are built from the same d.o.f. of the SM as gauge-invariant combinations under $\text{SU}(3)_C \times \text{SU}(2)_L \times \text{U}(1)_Y$ and C_i are the associated Wilson coefficients (WCs). In the following, we do not make any flavor symmetry assumption, therefore considering a completely general flavor scenario, for which the coefficients $[C_i]_J$ come with flavor indices J . Since we are dealing only with the first generation of leptons, we suppress such indices unless needed for clarity. Nevertheless, this flavor

assumption is crucial in global fits as it reduces the de-generation between coefficients entering the predictions for different processes.

The modified EW Lagrangian in the $\{\alpha, G_\mu, M_Z\}$ scheme reads as follows [78]

$$\begin{aligned} \mathcal{L}_{\text{SMEFT}}^{\text{EW}} = & -\sqrt{4\pi\alpha} (\bar{e}\gamma^\mu e) A_\mu \\ & + \frac{\sqrt{4\pi\alpha}}{s_w c_w} \left[\bar{e}_L \gamma^\mu \left(\hat{g}_L + \frac{\Delta g_L^{Ze}}{\Lambda_{\text{NP}}^2} \right) e_L \right. \\ & \left. + \bar{e}_R \gamma^\mu \left(\hat{g}_R + \frac{\Delta g_R^{Ze}}{\Lambda_{\text{NP}}^2} \right) e_R \right] Z_\mu, \end{aligned} \quad (9)$$

where A_μ and Z_μ are the photon and Z -boson field, respectively, and $e_{L,R}$ are the left- and right-handed electron fields. We neglect the operators $\hat{O}_{eW}^{(6)} = (\bar{e}_L \sigma^{\mu\nu} e_R) \sigma^I \phi W_{\mu\nu}^I$ and $\hat{O}_{eB}^{(6)} = (\bar{e}_L \sigma^{\mu\nu} e_R) \phi B_{\mu\nu}$, that generate dipole interactions after the Higgs acquires a vacuum expectation value v . The corresponding WCs $C_{eB,eW}$ are tightly constrained by lepton dipole moments [79, 80]. Moreover, their effect is suppressed by the electron Yukawa coupling y_e , yielding to a negligible contribution proportional to $v^2 y_e / \Lambda_{\text{NP}}^2$. In Eq. 9, the sine of the weak mixing angle is defined as $s_w^2 = \frac{1}{2} \left(1 - \sqrt{1 - 2\sqrt{2}\pi\alpha / G_\mu M_Z^2} \right)$. The effective shifts $\Delta g_{L(R)}^{Ze}$ parametrize the dimension-six SMEFT deviations from the SM left- and right-handed couplings of the Z boson to electrons, namely $\hat{g}_L = s_w^2 - 1/2$ and $\hat{g}_R = s_w^2$, see the first panel of Figure 3. Their expression in the Warsaw basis [81], given in the Appendix A, is a linear combinations of WCs acting as effective eeV couplings due to new interactions or modifications of the EW symmetry breaking entering the muon decay width when choosing G_μ as input [82]. At dimension six, also four-fermion contact interactions contribute to the Bhabha cross section, as shown in the second diagram in Fig. 3. Their Lagrangian is independent of the input scheme and reads as follows

$$\begin{aligned} \mathcal{L}_{\text{SMEFT}}^{\text{Af}} = & \frac{1}{2} \frac{C_{ll}}{\Lambda_{\text{NP}}^2} (\bar{e}_L \gamma^\mu e_L) (\bar{e}_L \gamma_\mu e_L) \\ & + \frac{C_{le}}{\Lambda_{\text{NP}}^2} (\bar{e}_L \gamma^\mu e_L) (\bar{e}_R \gamma_\mu e_R) \\ & + \frac{1}{2} \frac{C_{ee}}{\Lambda_{\text{NP}}^2} (\bar{e}_R \gamma^\mu e_R) (\bar{e}_R \gamma_\mu e_R), \end{aligned} \quad (10)$$

where the $1/2$ factors take into account the exchange of two identical currents.

At LO SMEFT, the prediction for the Bhabha cross section is given by

$$\sigma_{\text{SMEFT}} = \sigma_{\text{SM}} + \sigma^{(6)} = \sigma_{\text{SM}} + \sum_{i=1}^n \frac{C_i}{\Lambda_{\text{NP}}^2} \sigma_i^{(6)}, \quad (11)$$

where $\sigma_i^{(6)} = 2 \text{Re} \mathcal{M}_{\text{SM}}^\dagger \mathcal{M}_{\text{SMEFT},i}^{(6)}$ is the interference between the SM and SMEFT amplitudes due to the i th

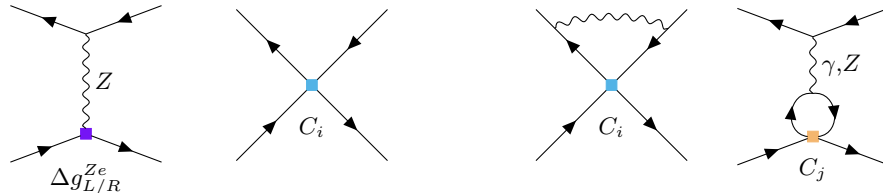


FIG. 3. Diagrams with insertion of SMEFT operators at dimension six, represented by square vertices. From the left to the right: the first diagram represents a shift of the Zee couplings in one of the two vertices. The second diagram is a four-fermion contact interaction. The latter two diagrams are NLO contribution: the first accounts for a virtual SM boson exchange on top of a four-fermion operator, and the rightmost represents a dimension-six NLO insertion. These diagrams are in interference with the SM ones in Fig. 1.

operator, having factored out the dependency on the ratio of the WCs to the NP scale and assuming they are real. We set $\Lambda_{\text{NP}} = 1 \text{ TeV}$, the EFT validity being ensured, as at small angle the relevant scale of the process is $\sqrt{|t|} = [s/2(1 - \cos\theta_{\min})]^{1/2}$, which is at most $\mathcal{O}(10^2) \text{ GeV}$ for $\sqrt{s} = 3 \text{ TeV}$ in the CLIC setup. We define the central deviation from the SM (differential) cross sections due to heavy NP and its 1σ uncertainty as

$$(\delta \pm \Delta\delta)_{\text{SMEFT}} = \frac{1}{\sigma_{\text{SM}}} \left(\sigma^{(6)} \pm \sqrt{\sum_{ij} \sigma_i^{(6)} V_{ij} \sigma_j^{(6)}} \right), \quad (12)$$

where the covariance matrix $V_{ij} = \Delta C_i \rho_{ij} \Delta C_j$ takes into account the correlation between fitted coefficients and their errors. We use the flavor-general bounds on coefficients and correlation matrix from the global fit of Ref. [78], that include EW and low-energy precision data. The values of WCs are reported in Table I whereas the

C_i	$C_i \pm \Delta(C_i)$
Δg_L^{Ze}	-0.0038 ± 0.0046
Δg_R^{Ze}	-0.0054 ± 0.0045
C_{ll}	0.17 ± 0.06
C_{le}	-0.037 ± 0.036
C_{ee}	0.034 ± 0.062

TABLE I. Central values and 68% uncertainty of the WCs, taken from the flavor general results of Eq. (4.8) in Ref. [78].

correlation matrix is given in the Appendix A. The shifts of the Zee couplings are well constrained yielding a negligible contribution to the SABS cross section; therefore, we consider only the impact of four-fermion operators. In Table II we show the uncertainty due to heavy NP deviation for SABS in the luminometer setup of future colliders. It can be seen that possible BSM effects would affect the luminosity precision target of future e^+e^- facilities in a non-negligible way [83]. With polarized beams at ILC and CLIC, we have checked that the results worsen up to a factor of 2, due to the enhancement of C_{ll} over C_{ee} . We have also checked that NP uncertainties were well below the precision goal of the luminosity determination at LEP with SABS, also by considering the bounds on

Exp.	$[\theta_{\min}, \theta_{\max}]$	$\sqrt{s} [\text{GeV}]$	$(\delta \pm \Delta\delta)_{\text{SMEFT}}$	$\Delta L/L$
FCC	$[3.7^\circ, 4.9^\circ]$	91	$(-4.2 \pm 1.7) \times 10^{-5}$	$< 10^{-4}$
		160	$(-1.3 \pm 0.5) \times 10^{-4}$	10^{-4}
		240	$(-2.9 \pm 1.2) \times 10^{-4}$	
		365	$(-6.7 \pm 2.7) \times 10^{-4}$	
ILC	$[1.7^\circ, 4.4^\circ]$	250	$(-1.2 \pm 0.5) \times 10^{-4}$	$< 10^{-3}$
		500	$(-4.9 \pm 1.9) \times 10^{-4}$	
CLIC	$[2.2^\circ, 7.7^\circ]$	1500	$(-9.7 \pm 3.9) \times 10^{-3}$	$< 10^{-2}$
		3000	$(-4.2 \pm 1.7) \times 10^{-2}$	

TABLE II. Heavy NP contamination to SABS as in Eq. (12) at future e^+e^- facilities. $\Delta L/L$ represents the luminosity target precision.

contact interactions given in [84]. At BELLE-II, which measures the machine luminosity using a large acceptance with Bhabha events, the effect is below the 10^{-3} precision budget.

In Figure 4 we show the differential behavior of the SMEFT correction as a function of the electron scattering angle, showing that the deviations grow with θ_e . This can be understood as the contact operators effect scales as $\delta_i^{4f} \simeq -sC_i(1 - \cos\theta)/(\Lambda_{\text{NP}}^2 2\pi\alpha)$ with respect to the SM one. When reducing the angular acceptance, for example lowering the maximum angle to $\theta_{\min} = 4.2^\circ$ in the $\sqrt{s} = 91 \text{ GeV}$ run of FCC-ee, the heavy NP contribution decreases to the -2×10^{-5} level, thus still representing a possible source of uncertainty.

At next-to-leading order (NLO) in the SMEFT the SABS prediction receives an additional contribution given by

$$\sigma_{\text{NLO}}^{(6)} = \sum_j \frac{C_j(\mu)}{16\pi^2 \Lambda_{\text{NP}}^2} 2 \text{Re} \left(\mathcal{M}_{\text{SM}}^\dagger \mathcal{M}_{\text{NLO},j}^{(6)}(\mu) \right) \quad (13)$$

where, in principle, the set of WCs entering the NLO prediction includes also operators not entering at LO accuracy. Systematic studies of NLO SMEFT corrections have been carried out for specific observables [85–89], while global analysis has been performed at (partial) NLO accuracy in the SMEFT and including the effects of renormalization group evolution (RGE) [90, 91]. We

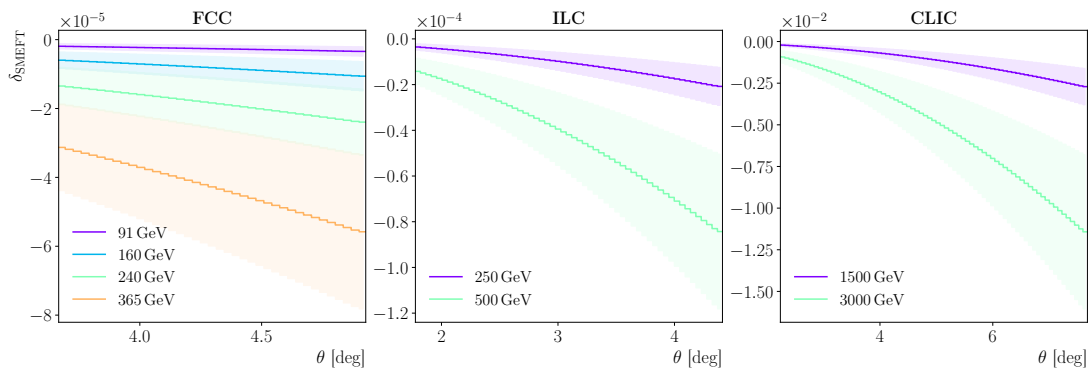


FIG. 4. SMEFT deviation to the SABS differential cross section as a function of the electron scattering angle in the same setup of Table II.

can estimate their effect on SABS by considering two different sets of contributions. The former case, depicted in the third panel in Fig. 3, is given by the NLO EW corrections to dimension-six operators and can be estimated as

$$\frac{\sigma_{\text{NLO},i}^{(6)}}{\sigma_{\text{LO},i}^{(6)}} \simeq \frac{g_{\text{SM}}^2}{16\pi^2} \log \frac{M_Z^2}{|t|}. \quad (14)$$

With t the typical scale of the SABS in the various setup and $\Lambda_{\text{NP}} \sim 1$ TeV, we conservatively get a contribution of the order of $\mathcal{O}(1\%)$ relative to the LO SMEFT prediction. The latter case concerns NLO insertions of \hat{O}_j operators not appearing at tree level, as shown in the last diagram in Fig. 3. They contribute to the SABS cross section as

$$\frac{\sigma_{\text{NLO},j}^{(6)}}{\sigma_{\text{SM}}^{(6)}} \simeq \frac{|t|}{\Lambda_{\text{NP}}^2} \frac{C_j}{16\pi^2} \log \frac{\Lambda_{\text{NP}}^2}{|t|}, \quad (15)$$

having chosen the renormalization scale as $\mu^2 = \Lambda_{\text{NP}}^2$. This effect is expected to be more relevant at high energies, yielding to a contribution of $2 \times 10^{-4} C_j$ with respect to the SM in the CLIC luminometer setup, while it is negligible in the other scenarios. Finally, RGE effects could give contributions of the same form of Eq (14), with the replacement $\log M_Z^2/|t| \rightarrow \log M_Z^2/\Lambda_{\text{NP}}^2$, which are roughly of the same order of magnitude. For these reasons, we can safely estimate the bulk of the SMEFT contribution as given by operators appearing only at LO and neglecting their radiative corrections, which play a useful role in constraining directions in global fits but are not expected to alter our conclusions.

The future HL-LHC data are not foreseen to further constrain significantly the four-electron WCs, as discussed, for example, in [91], in which the estimated reduction is of $\sim 20\%$ only. A possible strategy to remove the uncertainties induced by NP is to constrain the contact operators directly at future e^+e^- accelerators, by using observables that are independent of the absolute luminosity and can be measured with high precision.

III. CONSTRAINING CONTACT INTERACTIONS WITH LABS

In the worst-case scenario of no significant improvement on WCs bounds by the timeline of the start of future colliders, we explore in this section the possibility of constraining such coefficients. To this purpose, we rely on observables that do not depend on the luminosity and concern the LABS process, exploiting a phase-space region complementary to the SABS. Suitable quantities to this purpose are asymmetries, as they are defined as ratios and the luminosity dependence cancels out. They can be expressed in the following way:

$$A_{ab} = \frac{\sigma_a - \sigma_b}{\sigma_a + \sigma_b}, \quad (16)$$

where $\{a, b\} = \{\text{F}, \text{B}\}, \{\text{L}, \text{R}\}, \{\uparrow, \downarrow\}$ refer to different observables, as discussed in the following. The theoretical prediction for A_{ab} including the dimension-six SMEFT contribution can be written as

$$A_{ab}^{\text{th}} = A_{ab}^{\text{SM}} \left\{ 1 + \frac{(\sigma_a - \sigma_b)^{(6)}}{(\sigma_a - \sigma_b)_{\text{SM}}} - \frac{(\sigma_a + \sigma_b)^{(6)}}{(\sigma_a + \sigma_b)_{\text{SM}}} \right\}, \quad (17)$$

which depends on the WCs due to the definition of $\sigma_{a,b}^{(6)}$ given in Eq. (11). This dependence can be exploited by fitting the above expression with MC simulated data assumed to be a Gaussian $g(A_{ab}^{\text{SM}}, \Delta A_{ab})_{\alpha}$ centered about the SM tree-level prediction. The error is computed as

$$\Delta A_{ab} = \sqrt{\sum_{k=a,b} \left(\frac{\partial A_{ab}}{\partial N_k} \right)^2 \Delta_k^2} = 2 \sqrt{\frac{N_a N_b}{(N_a + N_b)^3}}, \quad (18)$$

assuming only statistical uncertainty $\Delta_k = \sqrt{N_k}$ on the number of events, given by the product of the time integrated luminosity and the cross section for the process $N_a = L\sigma_a$.

Therefore, if asymmetries related to the LABS process can be exploited, no additional assumptions on the NP scenarios are needed, allowing one to fit Eq. (17) with four-electron WCs. On the other hand, if one assumes

lepton flavor universality also asymmetries related to $\mu^+\mu^-$ and $\tau^+\tau^-$ pair production could be used, providing more constraining power. Throughout this section we consider conservatively the LABS in the $\theta \in [40^\circ, 140^\circ]$ acceptance, in analogy with the event selection conditions of LEP analyses [10]. This allows us to enhance the s -channel contribution to the Bhabha cross section and the sensitivity to the SMEFT parameters, with the aim of constraining the four-electron $\vec{C}_{4f} = (C_{ll}, C_{le}, C_{ee})$ coefficients. We assume the validity of the SM up to the starting of future colliders physics programs and focus on the attainable uncertainties of the WCs by future asymmetry data [92].

A. The Z resonance region

Around the Z peak, the natural asymmetry to be considered is the forward-backward asymmetry A_{FB} , which in s -channel processes is a key quantity for the measurement of electroweak couplings and parameters [3]. The A_{FB} of the LABS scattering is defined as in Eq (16) where

$$\sigma_{\text{F}} = 2\pi \int_0^c d \cos \theta \frac{d\sigma}{d\Omega} \quad \sigma_{\text{B}} = 2\pi \int_{-c}^0 d \cos \theta \frac{d\sigma}{d\Omega} \quad (19)$$

are the usual forward and backward cross sections where the acceptance cut is set to $c = \cos 40^\circ = 0.77$. The measurement of $A_{\text{FB}}(\sqrt{s})$ at three different values of \sqrt{s} can provide sufficient information to simultaneously constrain the three independent \vec{C}_{4f} coefficients. The three energy points more sensitive to deviations from the SM can be identified by calculating the difference between the prediction in the SM and in the SMEFT with current bounds on \vec{C}_{4f} , as shown in Fig. 5 and they are found as the two local minima located at $\sqrt{s_1} = 89$ GeV, $\sqrt{s_3} = 98$ GeV and the maximum at $\sqrt{s_2} = 93$ GeV. It is worth stressing that the radiative corrections will play an important role, in particular in the choice of the optimal energy points. Nevertheless we checked that, with the addition of QED leading logarithmic corrections switched on, the shape of the plot in Fig. 5 is preserved, the largest shift affecting the second local minimum which moves to about 103 GeV. By considering instead $\sqrt{s_3} = M_Z$ we still find enough constraining power on \vec{C}_{4f} .

The relative deviation of $A_{\text{FB}}(\sqrt{s_\alpha})$ in the SMEFT can be written by rearranging Eq (17) [93]

$$\sum_{i \in 4f} \frac{C_i}{\Lambda_{\text{NP}}^2} \left[\frac{(\sigma_{\text{F}} - \sigma_{\text{B}})_i^{(6)}}{(\sigma_{\text{F}} - \sigma_{\text{B}})_{\text{SM}}} - \frac{(\sigma_{\text{F}} + \sigma_{\text{B}})_i^{(6)}}{(\sigma_{\text{F}} + \sigma_{\text{B}})_{\text{SM}}} \right]_\alpha = \frac{\Delta A_{\text{FB},\alpha}^0}{A_{\text{FB},\alpha}^0}, \quad (20)$$

where the dependence on the WCs has been factored to the left while to the rhs we have the simulated data. To quantitatively estimate the uncertainty reduction for four-electron WCs at FCC-ee or CEPC, we solve the system of Eq. (20) by setting ΔA_{FB} to the foreseen experimental precision. Assuming six effective months of run

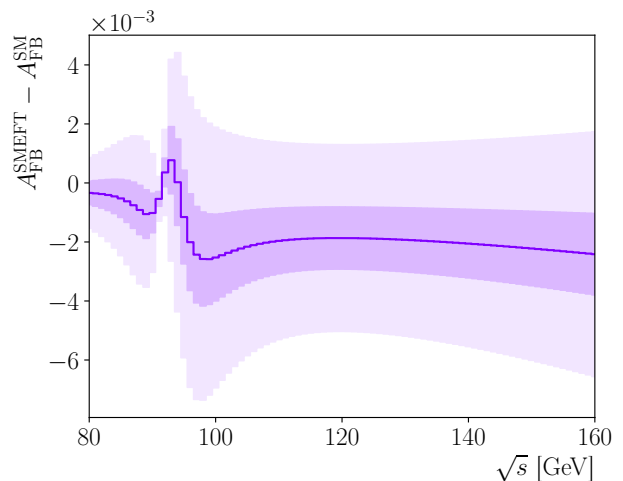


FIG. 5. Absolute deviation of the LABS A_{FB} predicted in the SMEFT and the SM, using the current knowledge on WCs. The solid line is the central value whereas the shaded regions are the 1σ and 3σ uncertainty bands.

(5×10^6 s) for each energy point with a FCC-like instantaneous luminosity $\mathcal{L}_{\text{FCC}} = 1.4 \times 10^{36} \text{ cm}^{-2} \text{ s}^{-1}$ [22], we find that the statistical uncertainty on the forward-backward asymmetry is $\Delta A_{\text{FB},\alpha}^0 \lesssim 5 \times 10^{-5}$. Therefore, the 1σ uncertainty on four-electron coefficients is reduced to $\Delta \vec{C}_{4f} \lesssim 10^{-2}$ yielding to a contribution $\delta_{\text{SMEFT}} \simeq 5 \times 10^{-6}$ on the Z -peak luminosity at FCC, which is smaller than the precision goal. This constraint would be enough also for future e^+e^- collider runs at higher energies.

B. The high-energy region

In the scenario of high-energy future machines that will not revisit the Z resonance scan, the A_{FB} observable can not be used to constrain the four-fermion WCs, as it is almost constant for $\sqrt{s} \gtrsim 120$ GeV. Since linear collider projects feature polarized beams, we investigate the possibility of using polarization asymmetries for LABS at $\sqrt{s} = 250$ GeV [94] at different angles assuming that they are independent of the luminosity [95]. For longitudinally polarized beams with fraction P_{e^\pm} of polarized positrons and electrons, the differential cross section in the scattering angle can be written as

$$\frac{d\sigma(P_{e^\pm})}{d \cos \theta} = \frac{1}{4} \sum_{I,J=L,R} (1 + P_{e_I^+})(1 + P_{e_J^-}) d\sigma_{e_I^+ e_J^-} \quad (21)$$

where $P_{e_R^\pm} = P_{e^\pm}$ and $P_{e_L^\pm} = -P_{e^\pm}$, with the proposed values $|P_{e^-}| = 0.8$ and $|P_{e^+}| = 0.3$. The theoretical prediction for polarization asymmetries $A_{\text{pol}}^{\text{th}}$, built from the SMEFT calculation of $d\sigma(P_{e^\pm})/d \cos \theta$ as defined in Eq. 21, can be exploited to fit the confidence intervals of \vec{C}_{4f} . We consider $n = 78$ experimental bins

in $\cos\theta$ of width $\Delta\cos\theta = 0.02$ and consider a multivariate Gaussian likelihood [93] whose negative logarithm $\chi^2 = -2\log L$ is defined as

$$\chi^2 = -2\log L = \sum_{\alpha=1}^n \frac{\left(A_{\text{pol}}^0 - A_{\text{pol}}^{\text{th}}(\vec{C}_{4f})\right)_{\alpha}^2}{(\Delta A_{\text{pol}}^0)_{\alpha}^2}, \quad (22)$$

which is distributed as a chi-squared with the number of d.o.f. given by $\nu = \dim(\vec{C}_{4f}) = 3$. The projected experimental value for the asymmetry in the β th bin and its statistical error $\Delta A_{\text{pol},\alpha}^0$ are computed as above, by taking an expected luminosity of $\mathcal{L}_{\text{ILC}} = 1.35 \times 10^{34} \text{ cm}^{-2} \text{ s}^{-1}$ for six months of run ($5 \times 10^6 \text{ s}$). $\chi^2(\vec{C}) = -2\log L(\vec{C})$. Under these hypotheses, the χ^2 can be rewritten as

$$\chi^2(\vec{C}) = \frac{1}{\Lambda_{\text{NP}}^4} \sum_{i,j} \sum_{\alpha,\beta} C_i \kappa_{i,\alpha}^{(6)} W_{\alpha\beta}^{-1} \kappa_{j,\beta}^{(6)} C_j,$$

where $\kappa_{i,\alpha}^{(6)} = \partial A_{\text{pol},\alpha}^{\text{th}} / \partial C_i$ is the derivative of the SMEFT theoretical prediction. The matrix $V_{ij}^{-1} = \sum_{\alpha,\beta} \kappa_{i,\alpha}^{(6)} W_{\alpha\beta}^{-1} \kappa_{j,\beta}^{(6)}$ is the inverse covariance matrix between WCs. The amplitude $\Delta(C_i)$ of the 68% confidence interval on C_i is given by $\sqrt{V_{ii}}$. This is equivalent to the projection on the C_i axis of the region in the space of WCs corresponding to $\chi^2(\vec{C}) \leq 1$, which we obtain with MC replicas.

The commonly measured left-right asymmetry is defined as $A_{\text{LR}}^{\text{ff}} = (\sigma_{\text{L}} - \sigma_{\text{R}}) / (\sigma_{\text{L}} + \sigma_{\text{R}})$, where the right cross section σ_{R} is obtained by measuring the quantity of Eq. (21) for a fixed set (P_{e^+}, P_{e^-}) and the left one σ_{L} is obtained by inverting the sign of the polarizations. This observable was used at the SLD experiment at SLC for a precision measurement of $\sin^2\theta_{\text{eff}}^{\ell}$ [96, 97] and it can be effective in future precision tests of the SM and of NP scenarios [28, 98–100]. Unfortunately, as shown in the third panel in Fig. 6, such asymmetry exhibits an almost exact flat direction as $C_{ll} \simeq C_{ee}$ due to its mild sensitivity to C_{le} , whose contribution depends on the product $P_{e^+}P_{e^-}$ and, hence, cancels in the numerator of A_{LR} . Therefore, in analogy with A_{LR} , we propose the following differential up-down asymmetry for a fixed \sqrt{s}

$$A_{\uparrow\downarrow}^{-}(P_{e^{\pm}}, \cos\theta) = \frac{d\sigma(P_{e^+}, P_{e^-}) - d\sigma(P_{e^+}, -P_{e^-})}{d\sigma(P_{e^+}, P_{e^-}) + d\sigma(P_{e^+}, -P_{e^-})}, \quad (23)$$

inverting the sign of P_{e^-} . In Fig. 6 we show the results of the χ^2 fit for $A_{\text{pol}} = A_{\text{LR}}, A_{\uparrow\downarrow}^{-}$ projected into 2D subspaces at 68% confidence level. While A_{LR} does not constrain further \vec{C}_{4f} , using the up-down asymmetry the uncertainty ΔC_i is reduced to a few 10^{-3} for all four-electron WCs. This would correspond to a negligible effect of $\delta_{\text{SMEFT}} \lesssim 10^{-7}$ on the SABS luminosity measurements.

IV. CONCLUSIONS

Assessing the NP contamination to luminosity measurements will be crucial to achieve the precision physics program at future e^+e^- colliders. In this paper, we have studied the BSM effects to the reference process SABS using an improved version of BABAYAGA@NLO.

We have shown that the impact of light new scalars and vectors on the absolute luminosity is well below the expected experimental uncertainties for all scenarios.

The heavy NP contributions have been parametrized in a model-independent way, within the SMEFT framework. We have shown that the shifts of the SM Zee couplings are irrelevant, whereas the uncertainties to the SABS due to four-electron operators are not negligible around the Z resonance, as well as at higher energies.

In order to reduce these uncertainties below the luminosity target precision, we have proposed to make use of the LABS process and to rely on observables that are independent of the absolute luminosity. We have shown quantitatively that the possible contamination around the Z peak can be removed by a measurement of A_{FB} at three different c.m. energy points close to the Z resonance. These measurements would be enough also for the removal of any possible bias to higher energies. In high-energy scenarios which do not foresee a run around the Z resonance, the forward-backward asymmetry is not useful anymore. However, high energy projects, like ILC and CLIC, feature beam polarization, which could allow to constrain the WCs by means of polarization asymmetries. In particular, we have shown that the measurement of the left-right asymmetry is not sufficient to constrain simultaneously the three four-electron operators. However, an asymmetry that flips only on beam polarization, named $A_{\uparrow\downarrow}$, has the necessary constraining power. The results of the present work could be put on firmer ground by including in our study the contribution of NLO corrections in the SM and SMEFT. This analysis is left to future work.

We also plan to further investigate the NP contamination to other relevant processes for precision luminosity monitoring at future lepton facilities, such as two-photon production in e^+e^- annihilation and $\mu^+\mu^- \rightarrow \mu^+\mu^-$ at a muon collider.

ACKNOWLEDGMENTS

We are indebted to Carlo M. Carloni Calame and Mauro Moretti for useful discussions. We thank Ilaria Brivio and Luca Mantani for helpful advice on SMEFT global fits and Marco Zaro for assistance with MG5_AMC@NLO. The authors are grateful to Alain Blondel, Roberto Tenchini, Graham Wilson and Dirk Zerwas for fruitful feedback on the experimental side. We also acknowledge Juan Alcaraz Maestre for interest in our work. C.L.D.P. is supported by the U.S. Department of Energy under Grant No. DE-SC0012704. F.P.

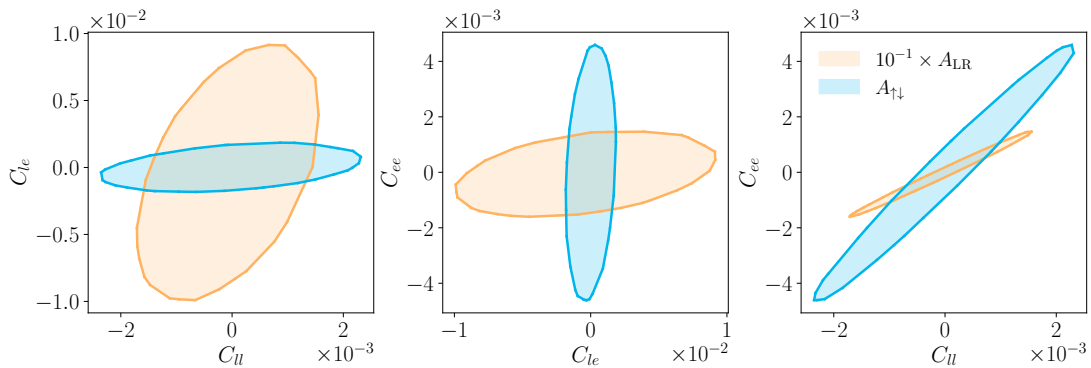


FIG. 6. Results of the χ^2 fit at 68% confidence level projected in two-dimensional subspaces. As can be seen in the third panel, the fit of A_{LR} manifests an approximate flat direction in the (C_u, C_{ee}) plane.

and F.P.U. thank the CERN theory department for hospitality during the completion of this work.

V. DATA AVAILABILITY

The data that support the findings of this article are not publicly available. The data are available from the authors upon request.

Appendix A: Details on Wilson Coefficients

In this appendix, we give further details on the WCs used in this work. We recall that the shifts to the Zee SM couplings are defined in terms of the Warsaw basis as [78]

$$\begin{aligned} \Delta g_L^{Ze} &= \frac{1}{\Lambda_{\text{NP}}^2} \left\{ -\frac{1}{2}[C_{HI}]_{11}^{(3)} - \frac{1}{2}[C_{HI}]_{11}^{(1)} + f\left(-\frac{1}{2}, -1\right) \right\} \\ \Delta g_R^{Ze} &= \frac{1}{\Lambda_{\text{NP}}^2} \left\{ -\frac{1}{2}[C_{HI}]_{11}^{(1)} + f(0, -1) \right\}, \end{aligned}$$

with

$$\begin{aligned} f(T^3, Q) &= -Q \frac{s_w c_w}{c_w^2 - s_w^2} C_{HWB} \\ &+ \left(\frac{1}{4}[C_U]_{1221} - \frac{1}{2}[C_{HI}^{(3)}]_{11} - \frac{1}{2}[C_{HI}^{(3)}]_{22} - \frac{1}{4}C_{HD} \right) \times \\ &\left(T^3 + Q \frac{s_w^2}{c_w^2 - s_w^2} \right), \end{aligned}$$

where T_3 and Q are the third component of the isospin and the charge of the electron, respectively, and the pedices indicate the flavor index $\{1, 2, 3\} = \{e, \mu, \tau\}$. The translation to other basis can be found in [101].

The correlation matrix between the shifts of the Z couplings to electrons $\Delta g_{L/R}^{Ze}$ and the four-electron coefficients \vec{C}_{4f} , whose numerical values are given in Table I, is given by

$$\rho = \begin{pmatrix} 1 & & & & \\ 0.15 & 1 & & & \\ -0.09 & -0.08 & 1 & & \\ 0.04 & -0.05 & -0.54 & 1 & \\ 0.08 & 0.08 & -0.04 & -0.54 & 1 \end{pmatrix}.$$

In this work we do not make any flavor hypothesis and use the results of [78]. By adopting instead the results from the global fit in [102], which assumes the more constraining $U(3)^5$ symmetry at high scale, the NP effect on the SABS cross section can be reduced approximately by a factor of 4, which is, however, not enough for the NP contamination to be below the precision goal at the future e^+e^- machines.

- [1] S. Actis *et al.* (Working Group on Radiative Corrections and Monte Carlo Generators for Low Energies), Quest for precision in hadronic cross sections at low energy: Monte Carlo tools vs. experimental data, Eur. Phys. J. C **66**, 585 (2010), arXiv:0912.0749 [hep-ph].
- [2] J. Altmann *et al.*, *ECFA Higgs, electroweak, and top*

- Factory Study*, CERN Yellow Reports: Monographs, Vol. 5/2025 (2025) arXiv:2506.15390 [hep-ex].
- [3] S. Schael *et al.* (ALEPH, DELPHI, L3, OPAL, SLD, LEP Electroweak Working Group, SLD Electroweak Group, SLD Heavy Flavour Group), Precision electroweak measurements on the Z resonance, Phys. Rept.

- 427**, 257 (2006), arXiv:hep-ex/0509008.
- [4] G. Voutsinas, E. Perez, M. Dam, and P. Janot, Beam-beam effects on the luminosity measurement at LEP and the number of light neutrino species, *Phys. Lett. B* **800**, 135068 (2020), arXiv:1908.01704 [hep-ex].
- [5] P. Janot and S. Jadach, Improved Bhabha cross section at LEP and the number of light neutrino species, *Phys. Lett. B* **803**, 135319 (2020), arXiv:1912.02067 [hep-ph].
- [6] P. Azzi, P. Azzurri, S. Biswas, F. Blekman, G. Corcella, S. D. Curtis, J. Erler, N. Foppiani, I. Heleinus, S. Jadach, P. Janot, F. Jegerlehner, P. Langacker, E. Locci, F. Margaroli, B. Mele, F. Piccinini, J. Reuter, M. Steinhauser, R. Tenchini, M. Vos, and C. Zhang, Physics behind precision, arXiv:1703.01626 [hep-ph].
- [7] P. Azzurri, The W mass and width measurement challenge at FCC-ee, *Eur. Phys. J. Plus* **136** (2021).
- [8] A. B. Arbuzov, V. S. Fadin, E. A. Kuraev, L. N. Lipatov, N. P. Merenkov, and L. G. Trentadue, Small angle Bhabha scattering for LEP 10.5170/CERN-1995-003.369 (1995).
- [9] G. Abbiendi *et al.* (OPAL Collaboration), Precision luminosity for Z^0 line shape measurements with a silicon tungsten calorimeter, *Eur. Phys. J. C* **14**, 373 (2000), arXiv:hep-ex/9910066.
- [10] G. Montagna, O. Nicosini, and F. Piccinini, Precision physics at LEP, *Riv. Nuovo Cim.* **21N9**, 1 (1998), arXiv:hep-ph/9802302.
- [11] J. de Blas *et al.*, Focus topics for the ECFA study on Higgs / Top / EW factories, arXiv:2401.07564 [hep-ph] (2024).
- [12] S. Jadach, W. Płaczek, M. Skrzypek, B. F. L. Ward, and S. A. Yost, The path to the 0.01% theoretical luminosity precision for the FCC-ee, *Phys. Lett. B* **790**, 314 (2019), arXiv:1812.01004 [hep-ph].
- [13] S. Abreu *et al.*, Theory for the FCC-ee: Report on the 11th FCC-ee Workshop Theory and Experiments, arXiv:1905.05078 [hep-ph] (2019).
- [14] B. F. L. Ward, S. Jadach, W. Placzek, M. Skrzypek, and S. A. Yost, Path to the 0.01% Theoretical Luminosity Precision Requirement for the FCC-ee (and ILC), in *International Workshop on Future Linear Colliders* (2019) arXiv:1902.05912 [hep-ph].
- [15] B. F. L. Ward, S. Jadach, W. Placzek, M. Skrzypek, and S. A. Yost, Overview of the Path to 0.01% Theoretical Luminosity Precision for the FCC-ee and Its Possible Synergistic Effects for Other FCC Precision Theory Requirements, *PoS ICHEP2020*, 704 (2021), arXiv:2012.11437 [hep-ph].
- [16] S. Jadach, W. Płaczek, M. Skrzypek, and B. F. L. Ward, Study of theoretical luminosity precision for electron colliders at higher energies, *Eur. Phys. J. C* **81**, 1047 (2021).
- [17] M. Skrzypek, W. Płaczek, B. F. L. Ward, and S. Y. Yost, How Well Could We Calculate Luminosity at FCCee?, *Acta Phys. Polon. Supp.* **17**, 2 (2024).
- [18] B. F. L. Ward, S. Jadach, W. Placzek, M. Skrzypek, and S. A. Yost, Outlook for the Theoretical Precision of the Luminosity at Future Lepton Colliders, *Proc. Sci. ICHEP2024* (2024), arXiv:2410.09095 [hep-ph].
- [19] J. A. Maestre, Precision studies of quantum electrodynamics at future e^+e^- colliders, arXiv:2206.07564 [hep-ph] (2022).
- [20] C. M. Carloni Calame, M. Chiesa, G. Montagna, O. Nicosini, and F. Piccinini, Electroweak corrections to $e^+e^- \rightarrow \gamma\gamma$ as a luminosity process at FCC-ee, *Phys. Lett. B* **798**, 134976 (2019), arXiv:1906.08056 [hep-ph].
- [21] M. Dam, Challenges for FCC-ee luminosity monitor design, *Eur. Phys. J. Plus* **137**, 81 (2022), arXiv:2107.12837 [physics.ins-det].
- [22] A. Abada *et al.* (FCC Collaboration), FCC Physics Opportunities: Future Circular Collider Conceptual Design Report Volume 1, *Eur. Phys. J. C* **79**, 474 (2019).
- [23] A. Abada *et al.* (FCC Collaboration), FCC-ee: The Lepton Collider: Future Circular Collider Conceptual Design Report Volume 2, *Eur. Phys. J. ST* **228**, 261 (2019).
- [24] M. Benedikt *et al.* (FCC Collaboration), Future Circular Collider Feasibility Study Report: Volume 1, Physics, Experiments, Detectors 10.17181/CERN.9DKX.TDH9 (2025), arXiv:2505.00272 [hep-ex].
- [25] CEPC Conceptual Design Report: Volume 1 - Accelerator, arXiv:1809.00285 [physics.acc-ph] (2018).
- [26] M. Dong *et al.* (CEPC Study Group), CEPC Conceptual Design Report: Volume 2 - Physics & Detector, arXiv:1811.10545 [hep-ex] (2018).
- [27] The International Linear Collider Technical Design Report - Volume 1: Executive Summary, arXiv:1306.6327 [physics.acc-ph] (2013).
- [28] The International Linear Collider Technical Design Report - Volume 2: Physics, arXiv:1306.6352 [hep-ph] (2013).
- [29] The International Linear Collider Technical Design Report - Volume 3.I: Accelerator & in the Technical Design Phase, arXiv:1306.6353 [physics.acc-ph] (2013).
- [30] The International Linear Collider Technical Design Report - Volume 3.II: Accelerator Baseline Design, arXiv:1306.6328 [physics.acc-ph] (2013).
- [31] H. Abramowicz *et al.*, The International Linear Collider Technical Design Report - Volume 4: Detectors, arXiv:1306.6329 [physics.ins-det] (2013).
- [32] I. B. Jelisić, S. Lukić, G. M. Dumbelović, M. Pandurović, and I. Smiljanić, Luminosity measurement at ilc, *Journal of Instrumentation* **8** (08), P08012–P08012.
- [33] Physics and Detectors at CLIC: CLIC Conceptual Design Report, arXiv:1202.5940 [physics.ins-det] (2012).
- [34] M. J. Boland *et al.* (CLIC, CLICdp), Updated baseline for a staged Compact Linear Collider, arXiv:1608.07537 [physics.acc-ph] (2016).
- [35] T. K. Charles *et al.* (CLICdp, CLIC), The Compact Linear Collider (CLIC) - 2018 Summary Report, arXiv:1812.06018 [physics.acc-ph] (2018).
- [36] H. Abramowicz *et al.*, A luminosity calorimeter for clic, <https://edms.cern.ch/document/1644637483> (Year), cERN EDMS Document 1644637483.
- [37] We remark that the fiducial volume for SABS events is smaller than the geometrical acceptance of the luminometer.
- [38] T. Hahn, Generating Feynman diagrams and amplitudes with FeynArts 3, *Comput. Phys. Commun.* **140**, 418 (2001), arXiv:hep-ph/0012260.
- [39] R. Mertig, M. Bohm, and A. Denner, FEYN CALC: Computer algebraic calculation of Feynman amplitudes, *Comput. Phys. Commun.* **64**, 345 (1991).
- [40] V. Shtabovenko, R. Mertig, and F. Orellana, New Developments in FeynCalc 9.0, *Comput. Phys. Commun.* **207**, 432 (2016), arXiv:1601.01167 [hep-ph].
- [41] L. Darmé *et al.*, UFO 2.0: the ‘Universal Feynman Output’ format, *Eur. Phys. J. C* **83**, 631 (2023),

- arXiv:2304.09883 [hep-ph].
- [42] A. Dedes, W. Materkowska, M. Paraskevas, J. Rosiek, and K. Suxho, Feynman rules for the Standard Model Effective Field Theory in R_ξ -gauges, *JHEP* **06**, 143, arXiv:1704.03888 [hep-ph].
- [43] A. Dedes, M. Paraskevas, J. Rosiek, K. Suxho, and L. Trifyllis, SmeftFR – Feynman rules generator for the Standard Model Effective Field Theory, *Comput. Phys. Commun.* **247**, 106931 (2020), arXiv:1904.03204 [hep-ph].
- [44] A. Dedes, J. Rosiek, M. Ryczkowski, K. Suxho, and L. Trifyllis, SmeftFR v3 – Feynman rules generator for the Standard Model Effective Field Theory, *Comput. Phys. Commun.* **294**, 108943 (2024), arXiv:2302.01353 [hep-ph].
- [45] I. Brivio, Y. Jiang, and M. Trott, The SMEFTsim package, theory and tools, *JHEP* **12**, 070, arXiv:1709.06492 [hep-ph].
- [46] I. Brivio, SMEFTsim 3.0 — a practical guide, *JHEP* **04**, 073, arXiv:2012.11343 [hep-ph].
- [47] J. Alwall, R. Frederix, S. Frixione, V. Hirschi, F. Maltoni, O. Mattelaer, H. S. Shao, T. Stelzer, P. Torrielli, and M. Zaro, The automated computation of tree-level and next-to-leading order differential cross sections, and their matching to parton shower simulations, *JHEP* **07**, 079, arXiv:1405.0301 [hep-ph].
- [48] A. Alloul, N. D. Christensen, C. Degrande, C. Duhr, and B. Fuks, FeynRules 2.0 - A complete toolbox for tree-level phenomenology, *Comput. Phys. Commun.* **185**, 2250 (2014), arXiv:1310.1921 [hep-ph].
- [49] The running code and all the results are available on GitHub.
- [50] C. M. Carloni Calame, C. Lunardini, G. Montagna, O. Nicrosini, and F. Piccinini, Large angle Bhabha scattering and luminosity at flavor factories, *Nucl. Phys. B* **584**, 459 (2000), arXiv:hep-ph/0003268.
- [51] C. M. Carloni Calame, An Improved parton shower algorithm in QED, *Phys. Lett. B* **520**, 16 (2001), arXiv:hep-ph/0103117.
- [52] G. Balossini, C. M. Carloni Calame, G. Montagna, O. Nicrosini, and F. Piccinini, Matching perturbative and parton shower corrections to Bhabha process at flavour factories, *Nucl. Phys. B* **758**, 227 (2006), arXiv:hep-ph/0607181.
- [53] G. Balossini, C. Bignamini, C. M. C. Calame, G. Montagna, O. Nicrosini, and F. Piccinini, Photon pair production at flavour factories with per mille accuracy, *Phys. Lett. B* **663**, 209 (2008), arXiv:0801.3360 [hep-ph].
- [54] E. Budassi, C. M. Carloni Calame, M. Ghilardi, A. Gurgone, G. Montagna, M. Moretti, O. Nicrosini, F. Piccinini, and F. P. Ucci, Pion pair production in e^+e^- annihilation at next-to-leading order matched to Parton Shower, *JHEP* **05**, 196, arXiv:2409.03469 [hep-ph].
- [55] A. Masiero, P. Paradisi, and M. Passera, New physics at the MUonE experiment at CERN, *Phys. Rev. D* **102**, 075013 (2020), arXiv:2002.05418 [hep-ph].
- [56] Y. M. Andreev *et al.* (NA64 Collaboration), Constraints on New Physics in Electron $g - 2$ from a Search for Invisible Decays of a Scalar, Pseudoscalar, Vector, and Axial Vector, *Phys. Rev. Lett.* **126**, 211802 (2021), arXiv:2102.01885 [hep-ex].
- [57] F. Acanfora, R. Franceschini, A. Mastroddi, and D. Redigolo, Fusing photons into nothing, a new search for invisible ALPs and Dark Matter at Belle II, *JHEP* **11**, 156, arXiv:2307.06369 [hep-ph].
- [58] F. Nguyen, F. Piccinini, and A. D. Polosa, $e^+e^- \rightarrow e^+e^-\pi^0\pi^0$ at DAPHNE, *Eur. Phys. J. C* **47**, 65 (2006), arXiv:hep-ph/0602205.
- [59] D. Babusci *et al.* (KLOE-2 Collaboration), Measurement of η meson production in $\gamma\gamma$ interactions and $\Gamma(\eta \rightarrow \gamma\gamma)$ with the KLOE detector, *JHEP* **01**, 119, arXiv:1211.1845 [hep-ex].
- [60] E. Budassi, C. M. Carloni Calame, C. L. Del Pio, and F. Piccinini, Single π^0 production in μe scattering at MUonE, *Phys. Lett. B* **829**, 137138 (2022), arXiv:2203.01639 [hep-ph].
- [61] S. J. Brodsky, T. Kinoshita, and H. Terazawa, Two Photon Mechanism of Particle Production by High-Energy Colliding Beams, *Phys. Rev. D* **4**, 1532 (1971).
- [62] M. Bauer, P. Foldenauer, and J. Jaeckel, Hunting All the Hidden Photons, *JHEP* **07**, 094, arXiv:1803.05466 [hep-ph].
- [63] N. Nath, N. Okada, S. Okada, D. Raut, and Q. Shafi, Light Z' and Dirac fermion dark matter in the $B - L$ model, *Eur. Phys. J. C* **82**, 864 (2022), arXiv:2112.08960 [hep-ph].
- [64] B. Holdom, Two $U(1)$'s and Epsilon Charge Shifts, *Phys. Lett. B* **166**, 196 (1986).
- [65] C. Boehm and P. Fayet, Scalar dark matter candidates, *Nucl. Phys. B* **683**, 219 (2004), arXiv:hep-ph/0305261.
- [66] M. Pospelov, A. Ritz, and M. B. Voloshin, Secluded WIMP Dark Matter, *Phys. Lett. B* **662**, 53 (2008), arXiv:0711.4866 [hep-ph].
- [67] J. P. Lees *et al.* (BaBar), Search for Invisible Decays of a Dark Photon Produced in e^+e^- Collisions at BaBar, *Phys. Rev. Lett.* **119**, 131804 (2017), arXiv:1702.03327 [hep-ex].
- [68] A. J. Krasznahorkay, M. Csatlós, L. Csige, Z. Gácsi, J. Gulyás, M. Hunyadi, T. J. Ketel, A. Krasznahorkay, I. Kuti, B. M. Nyakó, L. Stuhl, J. Timár, T. G. Tornyai, and Z. Vajta, Observation of anomalous internal pair creation in ^8Be : A possible signature of a light, neutral boson (2015), arXiv:1504.01527 [nucl-ex].
- [69] J. L. Feng, B. Fornal, I. Galon, S. Gardner, J. Smolinsky, T. M. P. Tait, and P. Tanedo, Protophobic fifth force interpretation of the observed anomaly in ^8Be nuclear transitions (2016), arXiv:1604.07411 [hep-ph].
- [70] A. J. Krasznahorkay, M. Csatlós, L. Csige, J. Gulyás, A. Krasznahorkay, B. M. Nyakó, I. Rajta, J. Timár, I. Vajda, and N. J. Sas, A new anomaly observed in ^4He supports the existence of the hypothetical x_{17} particle (2021), arXiv:2104.10075 [nucl-ex].
- [71] A. J. Krasznahorkay, A. Krasznahorkay, M. Begala, M. Csatlós, L. Csige, J. Gulyás, A. Krakó, J. Timár, I. Rajta, I. Vajda, and N. J. Sas, New anomaly observed in ^{12}C supports the existence and the vector character of the hypothetical x_{17} boson (2022), arXiv:2209.10795 [nucl-ex].
- [72] K. Afanaciev *et al.* (MEG II), Search for the X_{17} particle in $^7\text{Li}(p, e^+e^-)^8\text{Be}$ processes with the MEG II detector, (2024), arXiv:2411.07994 [nucl-ex].
- [73] F. B. et al., Search for a new 17 meV resonance via e^+e^- annihilation with the padme experiment (2025), arXiv:2505.24797 [hep-ex].
- [74] F. Arias-Aragón, G. G. di Cortona, E. Nardi, and C. Toni, Combined evidence for the x_{17} boson after padme results on resonant production in positron an-

- nihilation (2025), arXiv:2504.11439 [hep-ph].
- [75] D. Barducci, D. Germani, M. Nardecchia, S. Scacco, and C. Toni, On the atomki nuclear anomaly after the meg-ii result, *Journal of High Energy Physics* **2025**, 10.1007/jhep04(2025)035 (2025).
- [76] L. Di Luzio, P. Paradisi, and N. Selimovic, Hunting for a 17 MeV particle coupled to electrons, (2025), arXiv:2504.14014 [hep-ph].
- [77] I. Brivio and M. Trott, The Standard Model as an Effective Field Theory, *Phys. Rept.* **793**, 1 (2019), arXiv:1706.08945 [hep-ph].
- [78] A. Falkowski, M. González-Alonso, and K. Mimouni, Compilation of low-energy constraints on 4-fermion operators in the SMEFT, *JHEP* **08**, 123, arXiv:1706.03783 [hep-ph].
- [79] J. Aebischer, W. Dekens, E. E. Jenkins, A. V. Manohar, D. Sengupta, and P. Stoffer, Effective field theory interpretation of lepton magnetic and electric dipole moments, *JHEP* **07**, 107, arXiv:2102.08954 [hep-ph].
- [80] J. Kley, T. Theil, E. Venturini, and A. Weiler, Electric dipole moments at one-loop in the dimension-6 SMEFT, *Eur. Phys. J. C* **82**, 926 (2022), arXiv:2109.15085 [hep-ph].
- [81] B. Grzadkowski, M. Iskrzynski, M. Misiak, and J. Rosiek, Dimension-Six Terms in the Standard Model Lagrangian, *JHEP* **10**, 085, arXiv:1008.4884 [hep-ph].
- [82] We stress that if the electromagnetic coupling is not taken as an input also an overall $\Delta\alpha \neq 0$ shift is present at dimension six [46, 103].
- [83] We have verified that, by taking $\alpha(0)$ instead of $\alpha(M_Z)$ as input, the results change by a factor $\alpha(M_Z)/\alpha(0)$, which is well within the 68% error $\Delta\delta_{\text{SMEFT}}$.
- [84] S. Schael *et al.* (ALEPH, DELPHI, L3, OPAL, LEP Electroweak), Electroweak Measurements in Electron-Positron Collisions at W-Boson-Pair Energies at LEP, *Phys. Rept.* **532**, 119 (2013), arXiv:1302.3415 [hep-ex].
- [85] S. Dawson and P. P. Giardino, Electroweak and QCD corrections to Z and W pole observables in the standard model EFT, *Phys. Rev. D* **101**, 013001 (2020), arXiv:1909.02000 [hep-ph].
- [86] S. Dawson and P. P. Giardino, New physics through Drell-Yan standard model EFT measurements at NLO, *Phys. Rev. D* **104**, 073004 (2021), arXiv:2105.05852 [hep-ph].
- [87] K. Asteriadis, S. Dawson, P. P. Giardino, and R. Szafron, Impact of Next-to-Leading-Order Weak Standard-Model-Effective-Field-Theory Corrections in $e^+e^- \rightarrow ZH$, *Phys. Rev. Lett.* **133**, 231801 (2024), arXiv:2406.03557 [hep-ph].
- [88] K. Asteriadis, S. Dawson, P. P. Giardino, and R. Szafron, The $e^+e^- \rightarrow ZH$ Process in the SMEFT Beyond Leading Order, arXiv:2409.11466 [hep-ph] (2024).
- [89] S. Dawson, M. Forsslund, and P. P. Giardino, NLO SMEFT Electroweak Corrections to Higgs Decays to 4 Leptons in the Narrow Width Approximation, arXiv:2411.08952 [hep-ph] (2024).
- [90] R. Bartocci, A. Biekötter, and T. Hurth, Renormalisation group evolution effects on global SMEFT analyses, arXiv:2412.09674 [hep-ph] (2024).
- [91] E. Celada, T. Giani, J. ter Hoeve, L. Mantani, J. Rojo, A. N. Rossia, M. O. A. Thomas, and E. Vryonidou, Mapping the SMEFT at high-energy colliders: from LEP and the (HL-)LHC to the FCC-ee, *JHEP* **09**, 091, arXiv:2404.12809 [hep-ph].
- [92] Should the real data give values for the WCs not compatible with zero, this would be a clear indication of NP.
- [93] L. Berthier and M. Trott, Consistent constraints on the Standard Model Effective Field Theory, *JHEP* **02**, 069, arXiv:1508.05060 [hep-ph].
- [94] Since we are considering a large-angle observable, going to higher energies could spoil the validity of the EFT. A low/intermediate energy run would therefore be important for precision measurements.
- [95] K. Abe *et al.* (SLD), Precise measurement of the left-right cross-section asymmetry in Z boson production by e^+e^- collisions, *Phys. Rev. Lett.* **73**, 25 (1994), arXiv:hep-ex/9404001.
- [96] K. Abe *et al.* (SLD), Direct measurement of leptonic coupling asymmetries with polarized Z s, *Phys. Rev. Lett.* **79**, 804 (1997), arXiv:hep-ex/9704012.
- [97] K. Abe *et al.* (SLD), An Improved direct measurement of leptonic coupling asymmetries with polarized Z bosons, *Phys. Rev. Lett.* **86**, 1162 (2001), arXiv:hep-ex/0010015.
- [98] A. Aryshev *et al.* (ILC International Development Team), The International Linear Collider: Report to Snowmass 2021, arXiv:2203.07622 [physics.acc-ph] (2022).
- [99] S. Funatsu, H. Hatanaka, Y. Hosotani, Y. Orikasa, and N. Yamatsu, Bhabha scattering in the gauge-Higgs unification, *Phys. Rev. D* **106**, 015010 (2022), arXiv:2203.16030 [hep-ph].
- [100] C. Miller and J. M. Roney, Comparison of left-right asymmetry calculations in the Bhabha process at an upgraded SuperKEKB, arXiv:2411.16592 [hep-ph] (2024).
- [101] D. de Florian *et al.* (LHC Higgs Cross Section Working Group), Handbook of LHC Higgs Cross Sections: 4. Deciphering the Nature of the Higgs Sector, arXiv:1610.07922 [hep-ph] (2016).
- [102] R. Bartocci, A. Biekötter, and T. Hurth, A global analysis of the SMEFT under the minimal MFV assumption, *JHEP* **05**, 074, arXiv:2311.04963 [hep-ph].
- [103] A. Biekötter, B. D. Pecjak, D. J. Scott, and T. Smith, Electroweak input schemes and universal corrections in SMEFT, *JHEP* **07**, 115, arXiv:2305.03763 [hep-ph].